Segmentation of Brain MRI Based on Modified Type-2 Fuzzy Compactness

Tito G. Amaral*, V. Fernão Pires* ** ‡

*Department of Electrical Engineeering, ESTSetúbal, Instituto Politécnico de Setúbal, Setúbal, Portugal

**INESC-ID Lisboa, Portugal

(tito.amaral@estsetubal.ips.pt, vitor.pires@estsetubal.ips.pt)

‡Corresponding Author; V. Fernão Pires, Department of Electrical Engineering, EST Setúbal, Instituto Politécnico de Setúbal, Setúbal, Portugal, Tel: +351 265790000, vitor.pires@estsetubal.ips.pt

Received: 12.04.2025 Accepted: 17.06.2025

Abstract- One of the important aspects in many algorithms for image analysis, object representation and visualization is the image thresholding that is usually applied as an initial step. Another issue in image analysis is the segmentation since is an important image-processing step by which regions of an image are classified according to the presence of relevant anatomic features. The success of image segmentation depends on object-background intensity difference, object size and noise measurement, however is unaffected by location of the object on that image. In this context, this paper proposes a new automatic thresholding method to accurately segment the brain in magnetic resonance images (MRI) on the axial plane. The proposed automatic method is based on a new algorithm that utilizes a modified type-2 fuzzy compactness algorithm, allowing it to solve the global thresholding for brain MRI in the axial plane. Associated with this method it was used has metrics the Uniformity measure (UM) and Shape measure (SM) with the purpose to analyse their effectiveness. Experiment using real-image data of MR medical images demonstrated the accuracy and robustness of the proposed method. With the purpose to analyse the capability of the proposed method, it was realized a comparison with other two approaches, namely with the Otsu and Kittler methods. The obtained results of the proposed method achieved state-of-the-art results in which UM reaches 0.998 and SM reaches 1.000.

Keywords- MRI segmentation, uniformity measure, shape measure, global threshold, modified type-2 fuzzy compactness.

1. Introduction

In the field of biomedical image analysis has rapidly emerged over the last decades. The wide spread availability of suitable detectors have helped for the latest developments in medical analysis with respect to monitoring, diagnosing and treatment of the patients. Segmentation of brain Magnetic Resonance images (MRI) is a topic of great importance and much research in the field of medical imaging because of its excellent contrast of soft tissues and non-invasive characteristics. There are several segmentation methods available in the literature for the identification of the deformities with respect to the medical images pertaining to a patient's data. The image segmentation is used by radiologists in inspection of heart conditions by segmenting cardiac MRI data [1] and helping orthopaedists in the diagnosis and treatment of bone diseases [2]. In clinical routine, the method to segment both the endocardial and epicardial borders in 4D cine-MR images was also proposed [3]. However, manual segmentation of brain MRI is difficult and time consuming and can lead to errors due to low tissue contrast and unclear tissue boundaries caused by partial regions and operator interpretation.

One of the main techniques used in medical imaging is based on the segmentation, which is realized through the use of a method based on threshold segmentation. During the last decades, several thresholding methods have been developed. Several surveys have been made to categorize all these algorithms but since most algorithms use strategies of several groups this objective has been presented as a difficult task. From the several surveys, Lázaro present the binarization techniques divided into six groups [4]:

- Methods that make use of the histogram information namely peaks, valleys and curvatures.
- Methods that divide the image into clusters, one for the foreground (object) and the other for the background.
- Methods based on information theory to divide the image into object and background.

- Methods based on similarity measures between the original image and the binarized version of the image.
- Methods that find an optimal threshold value taking into account the spatial measures.
- Methods that find local thresholds instead of a global threshold for the entire image. The overall binarization of the original image is achieved by combining the thresholded subimages.

These methods can be manual, but also automatic. Thus, with the purpose to obtain an automatic segmentation of brain MRI, several methods have been proposed. Feng et all, proposed a multi-scale 3D Otsu thresholding algorithm for medical MR brain images [5]. The algorithm has an iteration procedure where the image is segmented by the 3D Otsu, and then filtered which will be the input into the next iteration. The final segmentation is obtained using majority voting rules of the partial segmentation results. However, when the histogram of the MR images is bimodal it is not possible to visualize the interior of the brain. Ilhan et all. presents an algorithm for the brain tumor segmentation using a threshold approach [6]. The algorithm segments the tumor region to be observed by the medical practitioner giving more detail about the tumor in their diagnosis. However, the proposed method is not an automatic procedure and it is not clear what the response of the algorithm is when there is no brain tumor. A comparative analysis on multilevel thresholding of MR brain image was presented by several works [7, 8]. However, in those cases the algorithms do not consider the global image thresholding. Some global segmentation methods were proposed but, in their evaluation, they do not use the shape measure to take into account the form of the segmented region for satisfying the human intuition on an "ideal" segmentation [9]. Other proposed segmentation approaches have been evaluated using metrics that require the gold standard labels or the ground truth images [10-12].

One of very interesting theories that appear and was applied to the thresholding was the Type-2 fuzzy logic. This theory began to appear up until the early 2000s and Tizhoosh used this type-2 fuzzy set theory in image thresholding [13]. However the author used the maximum of the ultrafuzziness measure to find the optimal threshold value in laser cladding images and create manually a gold standard (ground-truth image) to analyse the performance of his algorithm. If the ground-truth image it is not public than it is not possible to compare his results with other published works. Over the last years beyond the image segmentation the type-2 fuzzy concept was also applied in several image processing topics such as image enhancement [14], image filtering [15], image classification [16], image clustering [17] and edge detection [18]. For high-dimensional problems, [19] presented the extraction of fuzzy rule firings using a type-2 fuzzy neural network based on the Fourier transformation technique. The application of fuzzy theory in color space to identify color harmony patterns and dominant color palettes in images was explored by [20]. The inclusion of Type-2 fuzzy techniques in the fuzzy-based color model can be further studied, and their results should be analyzed.

In this paper, our contribution are as follows: 1) address the issue of automatic brain segmentation in T2-weighted MRI axial brain images, 2) propose a new algorithm based on a modified type-2 fuzzy compactness algorithm, allowing solving the global thresholding for brain MRI in the axial plane, 3) gain a state-of-the-art result.

To analyse the performance of the proposed algorithm it is used two well-known accuracy measures (uniformity and shape measures) that not depend of a manual interaction.

This paper is structured as follows: In Section 2, a detailed description relating to theoretical and implementation of the proposed method is provided. In Section 3 it is presented the accuracy measures used to analyse the performance of the proposed method. The test and the obtained results using real medical images are provided in Section 4 to verify the effectiveness of the proposed algorithm. Finally, some conclusions are summarized in the Section 5.

2. Proposed Method

In this section it is described the proposed method for thresholding the brain MR images. The proposed global thresholding algorithm uses the fuzzy index of compactness and the type-2 fuzzy sets to determine the global threshold value. The algorithm identified as Modified Type-2 Fuzzy Compactness uses the theory of fuzzy sets to determine iteratively some geometric properties allowing obtaining the global threshold value. The proposed algorithm includes two stages, as shown in Fig. 1. In the iterative stage the gray-level image is iteratively transformed in to the fuzzy domain and determined the area and the perimeter of the regions. After the computation of those two geometric properties, it is possible to determine the index of compactness which is a feature of the region's invariant to its translation, rotation and scale. In the thresholding stage the index of compactness is minimized and the global threshold value is calculated to obtain the final segmentation result.

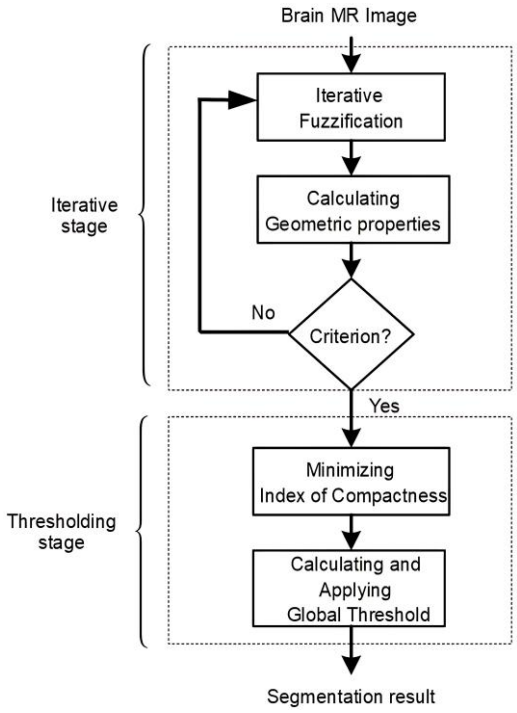

Fig. 1. Flowchart of the proposed method.

2.1 Iterative Fuzzification

In this stage the fuzzification procedure is an iterative process which will transform the colour of an image into its fuzzy domain. In order to define the type-2 fuzzy set it is necessary to select the type-1 membership function and assign the upper and lower membership degrees to construct the fuzzy set.

The type-1 membership function chosen was the standard S-function defined by (1) [21]. The cross-over point, b, and the bandwidth, Δb, are given by (2) and (3).

After selecting the initial type-1 membership function, μ_X, as the base of the fuzzy set then a practical definition for a type-2 fuzzy set, $\tilde{A}$, can be given by (4) [10].

$$\mu_X(x_{ij}) = S(x_{ij}, a, b, c) = \begin{cases} 0, & if\ x_{ij} \le a \\ 2\left(\frac{x_{ij}-a}{c-a}\right)^2, & if\ a \le x_{ij} \le b \\ 1-2\left(\frac{x_{ij}-c}{c-a}\right)^2, & if\ b \le x_{ij} \le c \\ 1, & if\ x_{ij} \ge c \end{cases} \quad (1)$$

$$b = \frac{(a+c)}{2} \quad (2)$$

$$\Delta b = b - a = c - b \quad (3)$$

$$\tilde{A} = \left\{ \left(x_{ij},\ \mu_{XU}(x_{ij}), \mu_{XL}(x_{ij})\right) \mid \forall x_{ij} \in X, \mu_{XL}(x_{ij}) \le \mu_X(x_{ij}) \le \mu_{XU}(x_{ij}), \mu \in [0,1] \right\} \quad (4)$$

In (4), the upper and lower membership functions, μ_{XU} and μ_{XL}, can be defined by the following linguistic hedges:

$$\mu_{XU}(x_{ij}) = \left[\mu_X(x_{ij})\right]^{1/\alpha} \quad (5)$$

$$\mu_{XL}(x_{ij}) = \left[\mu_X(x_{ij})\right]^{\alpha} \quad (6)$$

where $\alpha \in]1, \infty[$. Hedges generally appear as pairs which represent diagonally different modifications of the basic term. For different α values it is obtained distinct linguistic terms (shapes) such as dilation and concentration ($\alpha = 2$) or deaccentuation and accentuation ($\alpha = 1.75$).

Considering a gray level image X, the degree of brightness of each pixel in the fuzzy domain, $\mu_{\tilde{A}}(x_{ij})$, can be determined by (7).

$$\mu_{\tilde{A}}(x_{ij}) = abs\left(\mu_{XU}(x_{ij}) - \mu_{XL}(x_{ij})\right) \quad (7)$$

The fuzzy domain is also called by footprint of uncertainty (FOU) which is the region between the pair of hedges. The cross-over point, the bandwidth and the shape parameters are iteratively modified in order to find the best values for a good segmentation result.

As an example, considering the values of cross-over point and bandwidth are equal to 127 and the linguistic terms dilation and concentration, then using (5) and (6), it will be obtained the type-2 S-function represented in Fig.2. Considering these values, the relation between the degree of brightness of each pixel in the fuzzy domain and the intensity levels in the gray level image is represented in Fig.3.

Despite of the cross-over point is always in the middle of the interval between a and c points in the type-1 S-function the type-2 S-function is not symmetric. However, is symmetric the relation between the intensity levels in the gray level image, X, and the type-2 fuzzy domain around $\mu_{\tilde{A}}(x_{ij}) \cong 0.5$.

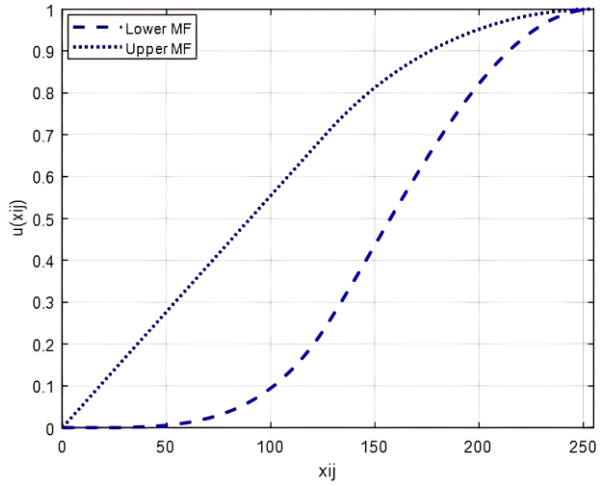

Fig. 2. Type-2 S-function.

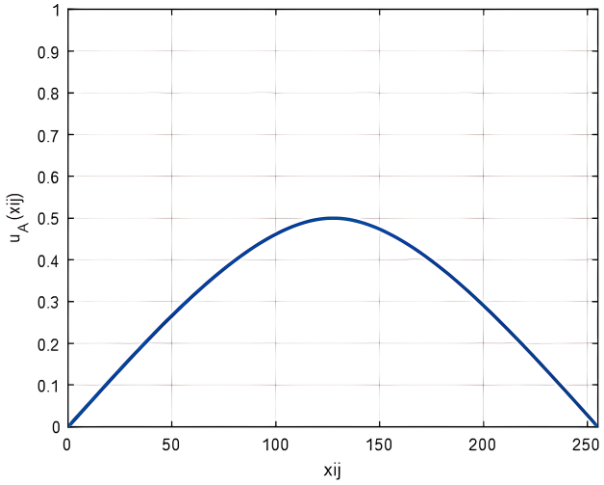

Fig. 3. Intensity levels in the type-2 fuzzy domain.

By changing the values of cross over point, bandwidth and shape, different values of the geometric properties are obtained, resulting in different segmented images. When b, Δb and α corresponds to the appropriate threshold between two regions there will be a minimum number of pixel intensities in X having $\mu_{\tilde{A}}(x_{ij}) \cong 0.5$ and a maximum number of pixel intensities having $\mu_{\tilde{A}}(x_{ij}) \cong 0$. The flexibility of the type-2 membership function is the key issue of the proposed algorithm identified as Modified Type-2 Fuzzy Compactness Algorithm.

2.2 Geometric Properties Calculation

The proposed method for the automatic segmentation of the brain MRI, will be based on the Rosenfeld extended concept of the standard geometric properties and relationships among regions to fuzzy subsets [22]. Among the extensions of the various properties, it will enter into consideration with the area, the perimeter and the compactness of a fuzzy image subset, characterized by $\mu_{\tilde{A}}(X_{mn})$. This is fundamental in the method, as will be described in the following sections, since will determine the global threshold value. For definition of the area, perimeter and compactness, $\mu_{\tilde{A}}(X_{mn})$ is replaced by μ for simplicity.

The area of μ is defined as the weighted sum of the areas of the regions on which μ has constant values, weighted by these values (8).

$$A(\mu) = \sum_i \sum_j \mu(i,j) \tag{8}$$

For the piecewise constant case, the perimeter of μ is defined as the weighted sum of the length of the arcs along which the i^{th} and j^{th} regions having constant values μ_i and μ_j respectively meets, weighted by the absolute difference of these values (9).

$$\begin{aligned} P(\mu) \equiv & \sum_{i,j} \sum_k |\mu_i - \mu_j| |A_{ijk}| \\ & i,j = 1,2,\dots,r; \\ & i < j; \\ & k = 1,2,\dots,r_{ij} \end{aligned} \tag{9}$$

The index of compactness of a fuzzy image, μ, is defined by:

$$IOC(\mu) = \frac{A(\mu)}{P^2(\mu)} \tag{10}$$

In the proposed work for the determination of the global threshold value it is used the minimization of the index of compactness since for fuzzy regions this index is smallest for its crisp version.

2.3 Index of Compactness Minimization

For each position of the S-function it is determined the three geometric properties described in the previous section. The number of different positions of the S-function depends on the difference between the maximum and minimum of the image gray-level. Considering l_{sup} and l_{inf} the higher and lower gray-level values of the X image, the minimization of the index of compactness is given by:

$$\begin{aligned} IOC_{opt} = & \min\left(IOC(a_i, \Delta b_j)\right), \\ & i = l_{inf}, \dots, l_{sup} - \Delta b_j; \\ & j = 2, \dots, l_{sup} - l_{inf.} \end{aligned} \tag{11}$$

2.4 Global Threshold Calculation

The S-function that presents the minimum value of the index of compactness permits to obtain the optimum value of the cross-over point, b_{opt} and bandwidth, Δb_{opt}. The optimum cross-over point corresponds to the threshold value used to segment the image in its two-tone version (12).

$$X_{bw}(i,j) = \begin{cases} 1, & if\ \mu(i,j) > b_{opt} \\ 0, & otherwise \end{cases} \tag{12}$$

2.5 Proposed Modified Type-2 Fuzzy Compactness Algorithm

With the objective to describe the proposed algorithm, it will be considered a generic image X with dimension $M \times N$ having the minimum and maximum gray levels l_{min} and l_{max}. Thus, in accordance with this, the algorithm will be defined in several points, as following described:

1- Obtain the degree of brightness, $\mu_X(x_{ij})$ using (1) where;

$$\mu_X(x_{ij}) = S(x_{ij}, a_i, a_i + \Delta b_i, a_i + 2\,\Delta b_i) \tag{13}$$

2- Obtain the type-2 fuzzy set, $\tilde{A}$, determining the upper and lower membership functions, μ_{XU} and μ_{XL}, using (5) and (6) where;

$$\begin{aligned} \mu_{XU}(x_{ij}) = f(S(x_{ij}, a_i, a_i + \Delta b_i, a_i \\ + 2\,\Delta b_i), 1/\alpha_i) \end{aligned} \tag{14}$$

$$\begin{aligned} \mu_{XL}(x_{ij}) = f(S(x_{ij}, a_i, a_i + \Delta b_i, a_i \\ + 2\,\Delta b_i), \alpha_i) \end{aligned} \tag{15}$$

3- For each a_i, Δb_i and α_i determine the type-2 fuzzy domain, $\mu_{\tilde{A}}(x_{ij})$, using (7).

4- Compute the correspondent area and perimeter of $\mu_{\tilde{A}}(x_{ij})$

$$A(\mu_{\tilde{A}}) = \sum_{i=1}^{M} \sum_{j=1}^{N} \mu_{\tilde{A}}(x_{ij}) \tag{16}$$

and

$$\begin{aligned} P(\mu_{\tilde{A}}) = & \sum_{i=1}^{M} \sum_{j=1}^{N-1} |\mu_{\tilde{A}}(x_{ij}) - \mu_{\tilde{A}}(x_{i,j+1})| \\ & + \sum_{j=1}^{N} \sum_{i=1}^{M-1} |\mu_{\tilde{A}}(x_{ij}) \\ & - \mu_{\tilde{A}}(x_{i+1,j})| \end{aligned} \tag{17}$$

5- Determine the compactness in $\mu_X(x_{mn})$ with

$$IOC(\mu_{\tilde{A}}) = \frac{A(\mu_{\tilde{A}})}{P^2(\mu_{\tilde{A}})} \tag{18}$$

6- Vary a_i from l_{min} to $l_{max} - \Delta b_i$;

7- Vary α_i from 1.25 to 4;

8- Vary Δb_i from 2 to $l_{max} - l_{min}$;

9- Select the global threshold, $th = a_i + \frac{\Delta b_i}{2}$ for which the $IOC(\mu_{\tilde{A}})$ obtained is minimum value.

Figure 4(a) shows the variation of the cross-over point in the type-2 S-function for the same bandwidth and linguistic terms, Δb and α. The variation of the bandwidth in the type-2 S-function is represented in Fig.4(b). The effect of the change in the linguistic terms in the type-2 fuzzy domain is shown in Fig.5.

The threshold value, th, denotes the cross-over point and bandwidth of the brightness image $\mu_{\tilde{A}}(x_{ij})$ which is most crisp. The obtained $\mu_{\tilde{A}}(x_{ij})$ can be viewed as a fuzzy segmented image of X and the parameter th is considered the threshold value for segmenting the image into regions.

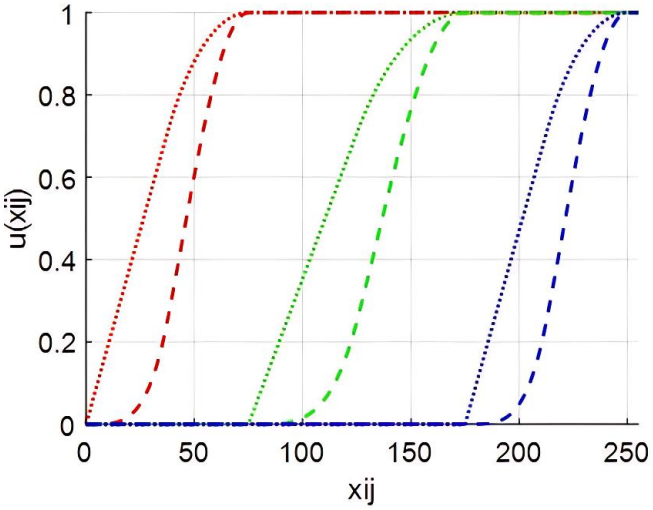

Fig. 4 (a). Type-2 S-function with constant bandwidth and shape.

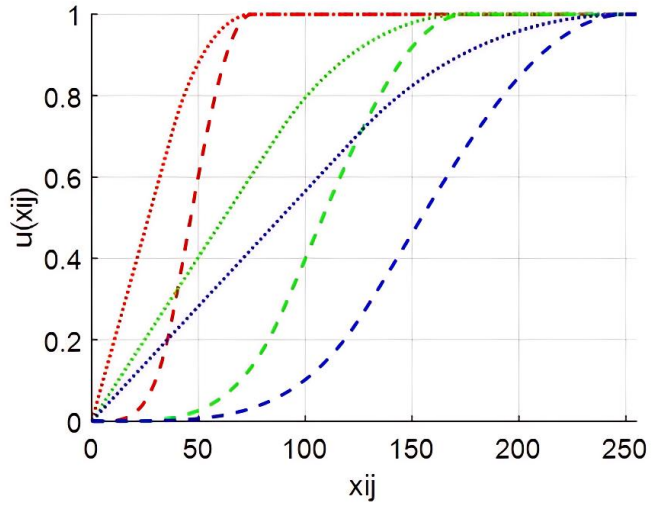

Fig. 4 (b). Type-2 S-function with different bandwidths.

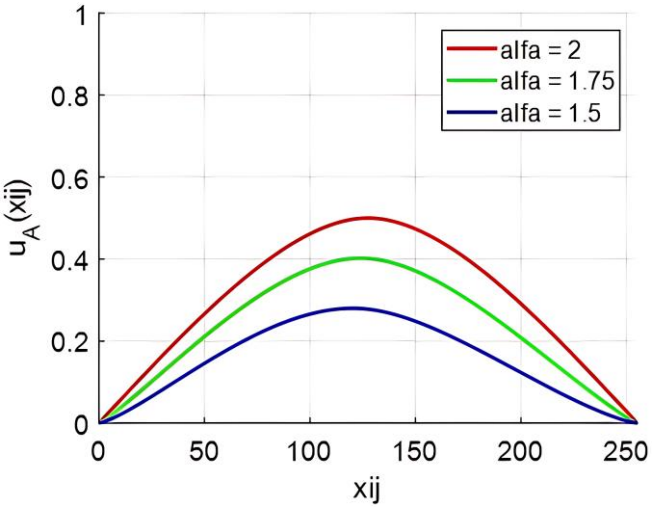

Fig. 5. Type-2 Fuzzy domain for different linguistic terms.

3. Accuracy Measurement of Image Segmentation

In order to gain a better understanding of a good image segmentation avoiding errors that could appears by visual analysis, extensive research have been carried out by creating many different approaches and algorithms. However, it is still difficult to assess whether one algorithm produces more accurate segmentation than another one [23]. Image segmentation partitions the entire image region *R* into many sub regions where every region is partially connected and every pixel belonging to only one region satisfies a specified similarity predicate [24].

Many works evaluate the performance of the methods only by visual inspection [25, 26]. However, this is not a reliable way of analysing the performance of the method under study. For the used MRI brain images, the medical ground truth of segmentation is not available. In the absence of such ground truth and in order to evaluate the performance of the proposed algorithm and compare with two of the most known used methods (Otsu method and Kittler method) it will be used the uniformity measure [27, 30] and shape measure [31, 32].

The uniformity measure is used to describe the homogeneity of a region in an image. For an image segmented using a global threshold, the uniformity measure is defined as,

$$u = 1 - 2 \cdot \frac{\sum_{j=0}^{p} \sum_{j \in R_j} (f_i - \mu_j)^2}{N \cdot (f_{max} - f_{min})^2} \quad (19)$$

$$\mu_j = \frac{1}{N_j} \sum_{j \epsilon R_j} f_i \quad (20)$$

where;

R_j	jth segmented region,
N	total number of pixels in the given image,
N_j	number of pixels in the jth segmented region
f_i	gray level of pixel i,
μ_j	mean gray level of pixels in jth region,
f_{max}	maximum gray level of pixels in the given image,
f_{min}	minimum gray level of pixels in the given image.

The value of the uniformity measure, u, should lie between 0 and 1. A higher value of u indicates that there is better uniformity in the thresholded image and better quality of thresholding.

Conversely a lower value of u indicates worse quality of the thresholding procedure. The shape measure is used to measure geometric features of regions present in an image. The shape measure is given by:

$$S = \frac{\sum_{(x,y)\epsilon R_j} sign(I(x,y) - I_N)\, \Delta(x,y)\, sign(I(x,y) - th)}{C} \tag{21}$$

where the parameter *th* is the optimal threshold value obtained according to each method and the generalised gradient function, Δ(x,y), is defined by:

$$\Delta(x,y) = \left[\sum_{k=1}^{4} D_k^2 + \sqrt{2}\, D_1\, (D_3 + D_4) - \sqrt{2}\, D_2\, (D_3 - D_4)\right]^{\frac{1}{2}} \tag{22}$$

The gradient into four directions is determined by the following expressions:

$$D_1 = I(x+1,y) - I(x-1,y) \tag{23}$$

$$D_2 = I(x,y-1) - I(x,y+1) \tag{24}$$

$$D_3 = I(x+1,y+1) - I(x-1,y-1) \tag{25}$$

$$D_4 = I(x+1,y-1) - I(x-1,y+1) \tag{26}$$

The gradient D1 represent the gray-level changes along x-axis (i.e., 0º–180º), whereas the gradient D2 represent the gray-level changes along the y-axis (i.e., 90º–270º). In the same way, the gradients D3 and D4 represent the gray-level changes diagonally (i.e., 45º–225º) and anti-diagonally (i.e., 135º–315º), respectively. The boundary of the image is omitted in this measure since there are pixels that aren't in the interior of the thresholded region. The average gray value in the neighbourhood $N(x,y)$ is determined by:

$$I_{N(x,y)} = \frac{1}{8}\left[\left(\sum_{i=x-1}^{x+1}\sum_{j=y-1}^{y+1} I(i,j)\right) - I(x,y)\right] \tag{27}$$

where the sign function is given by:

$$sign(x) = \begin{cases} 1 & if\ x \geq 0 \\ -1 & if\ x < 0 \end{cases} \tag{28}$$

The normalisation factor is used to limit the shape measure in the range [0 1] and is given by [32]

$$C = \max_{t}\left\{\sum_{(x,y)\epsilon R_j} sign(I(x,y) - I_N)\, \Delta(x,y)\, sign(I(x,y) - th)\right\} \tag{29}$$

The uniformity and shape measures are the best-known objective evaluation criteria for evaluating the performance of image segmentation, and many literatures use the two criteria to judge the merits of the image segmentation methods [34, 35]. In this paper, the uniformity and the shape values are obtained at the optimal threshold values of various algorithms.

4. Results and Discussion

As referred previously, in this study, it is proposed a segmentation method for brain MRI images. The performance evaluation of the proposed algorithm is applied to medical brain images which are freely available on the website of the Harvard Medical School [36] and are widely used [8, 29, 30]. From the available images, it was chosen T2-weighted MRI axial brain images with ten slices as shown in Fig.6 for segmentation. Each image is of 256x256 size and each of these gray-level images has 8-bit representations of their intensity levels corresponding to L=256 gray levels. Considering a normal tissue, the dark regions have low signal intensity and correspond to dense bones or air regions. The bright regions have high signal intensity and correspond to fat or cerebrospinal fluid. Regions with intermediate colours correspond to the white matter, gray matter. The abnormal tissue in the MR-T2 appears normally has a bright region. Since the MR medical images used in this study aren't raw images, they already don't have inherently conspicuous noise. When MR images present this type of noise it is used normally the Sigma filter which is computational efficient and with the ability to retain subtle details, preserving edge shapes [37]. In order to make the study more complete, the results obtained by the proposed modified fuzzy compactness method will be compared with the ones obtained by Otsu's method [38] and by Kittler method [39]. Otsu's method is a widely used thresholding method that finds the optimal threshold value by maximizing the between-class variance of gray levels. The Kittler method was considered by Sezgin the best thresholding method of a set of forty methods [40]. This method finds the minimum error thresholding assuming that the object and pixel gray level values are normally distributed. One problem faced by many of the thresholding techniques is the fact that several images with the same histogram yield the same threshold. The two methods selected to compare the results with those results obtained by the proposed method doesn't suffer from that problem. All the methods are implemented using MATLAB2022b and the simulation are carried out using Intel Core i7-1280P processor with CPU 2.00 GHz, 16 GB RAM and with the operating system 64-bit Windows 11. The code that was developed for the proposed approach is available on GitHub at:
https://github.com/TGBA68/Modified-Type-2-Fuzzy-Compactness

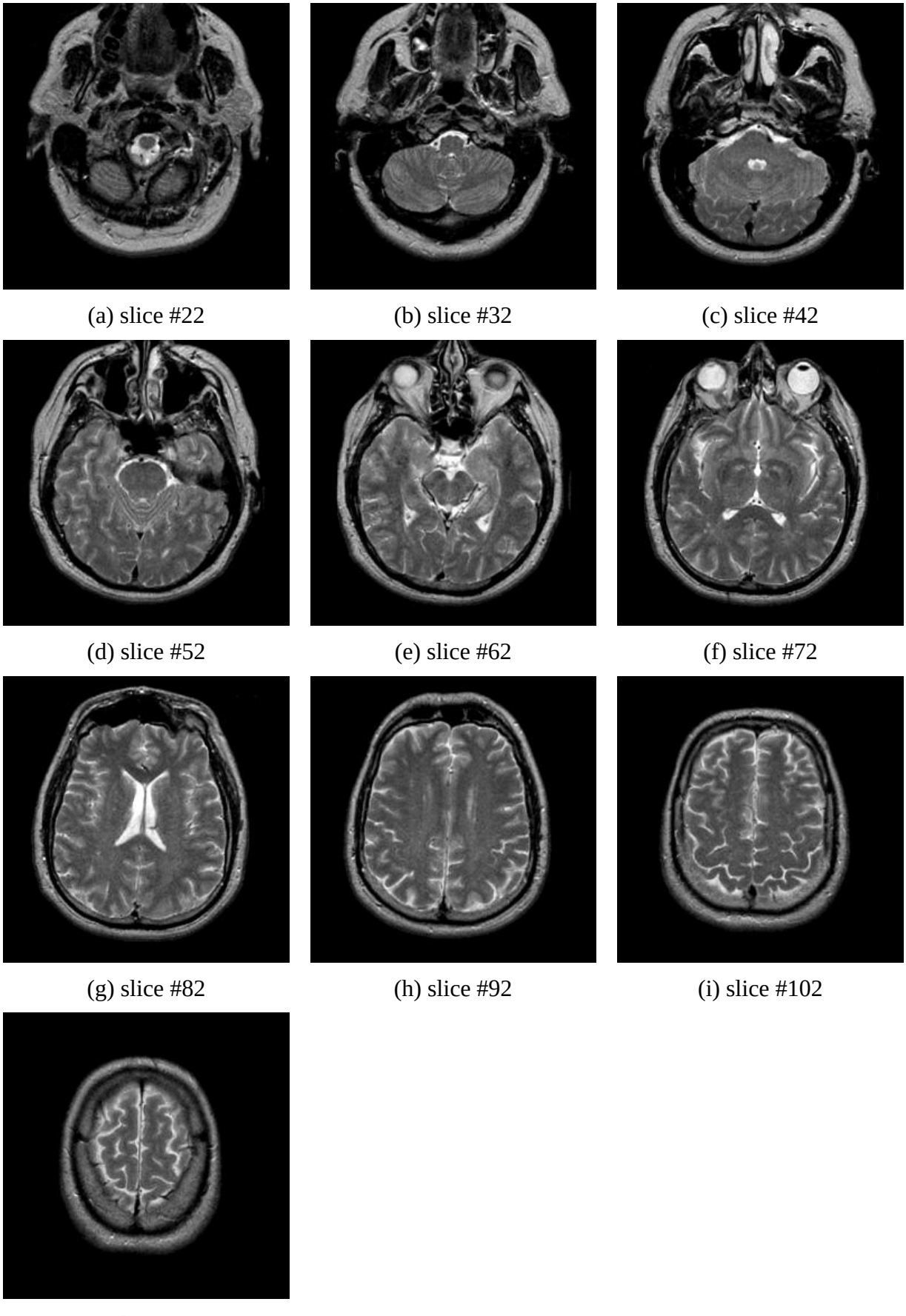

(a) slice #22 (b) slice #32 (c) slice #42

(d) slice #52 (e) slice #62 (f) slice #72

(g) slice #82 (h) slice #92 (i) slice #102

(j) slice #112

Fig. 6. MR-T2 brain slices.

The computational cost of the proposed algorithm depends on the considered number of different crossovers point positions, and for each position, it also depends on the bandwidth ranges and the different linguistic terms considered in the iterative fuzzification stage. Considering the possibility of four different linguistic terms and 253 different bandwidth ranges, with a total of 129,540 crossover point positions, the average processing time of the proposed algorithm is 3.4 seconds. However, it should be noted that there was no concern about optimizing the respective code. The segmentation accuracy of the medical image is evaluated by the uniformity and shape measures. To the higher value of those measures, it corresponds a better accuracy of the image threshold. Table 1 show the results by the application of the uniformity measure to the images under study where the best values are marked in bold. From this evaluation is possible to verify that Kittler method presents a slightly better thresholding method when compared with the proposed method and Otsu method. Table 2 show the results obtained using the shape measure applied to the same images. The proposed method outperforms the Otsu method for all the slices except the first two slices. The Kittler method has a shape accuracy measure significantly lower than the other two methods.

Table 1. Evaluation results using uniformity measure

Testing images	Uniformity measure		
	Proposed method	Otsu's method	Kittler method
slice #22	0.9983	0.9980	**0.9984**
slice #32	0.9978	0.9981	**0.9983**
slice #42	0.9978	0.9983	**0.9985**
slice #52	0.9979	0.9983	**0.9984**
slice #62	0.9977	0.9982	**0.9984**
slice #72	0.9979	0.9984	**0.9986**
slice #82	0.9979	0.9986	**0.9987**
slice #92	0.9980	**0.9987**	**0.9987**
slice #102	0.9982	0.9987	**0.9988**
slice #112	0.9984	0.9989	**0.9990**

Table 2. Evaluation results using shape measure

Testing images	Shape measure		
	Proposed method	Otsu's method	Kittler method
slice #22	0.6469	**1.0000**	0.2057
slice #32	0.9994	**1.0000**	0.1565
slice #42	**1.0000**	0.9811	0.1950
slice #52	**1.0000**	0.8603	0.1536
slice #62	**1.0000**	0.8519	0.1517
slice #72	**1.0000**	0.7493	0.1131
slice #82	**1.0000**	0.7714	0.1113
slice #92	**1.0000**	0.7759	0.1086
slice #102	**1.0000**	0.7438	-0.0605
slice #112	**1.0000**	0.6681	-0.1122

Table 3 presents the gray levels which optimize the uniformity and shape measure for the MR brain images. The proposed method and the Otsu method give a biased threshold value when compared with kittler method. This was expected and the reason was already discussed by Kittler [41]. Observing the threshold values obtained using the proposed method, it verify that the value obtained for slice #22 is very different from the remaining threshold values obtained for all the other slices. This is due to the contrast difference between this slice and all the other slices in analysis. It can also be seen that excepting for the slice #22 the threshold values obtained by Otsu method are always lower than the correspondent values obtained by the proposed method.

The threshold images obtained by the three methods are showed in Fig.7. Thus, from the visual aspect of the binary images, it is possible to verify that Otsu method presents itself as the best thresholding method for slices #22 to #32 and the proposed method for the slices #42 to #112. However, the binary images obtained by the Kittler method for all the slices do not allow distinguishing the various regions that exists in the brain.

From Fig.7 it can be seen that the Otsu method doesn't correctly segment the region of the brainstem (slices #52 and #62) and has much difficult to distinguish between the white matter and gray matter (slices #72 to #112). This can be confirmed by the histograms of the brain slices represented in Fig.8. When the brain image does not have a distinct bimodal gray-level histogram then the Otsu method ranks first according to shape measure and uniformity measure when compared with the proposed method.

From Fig.8 it can be seen that the histogram of the slice #22 does not present a clear bimodal shape. The histogram of the slices #32 and #42 starts to present slightly a bimodal shape and the obtained results of the proposed method approaches from those obtained by Otsu method. Thus, for the brain image which has a bimodal histogram, the proposed method is found to be a best method if only the shape measure is considered, whereas the Kittler method is the best one on the basis of uniformity measure alone. However, although the uniformity values obtained by the three methods are very close, the respective binary images are very different.

The Kittler method searches for an internal minimum of the criterion function to find the optimum threshold. If the internal and unique minimum is found it means that the image has a bimodal histogram. However, the absence of an internal minimum indicates a unimodal histogram corresponding to a homogeneous image. If the image to be threshold is homogeneous or the Kittler method found a local minimum in the boundaries of the interval of the gray level values of the image then the binarization results is inappropriate. The last situation is the one that happens resulting in an inefficient binarization from the visual point of view.

The shape measurement values obtained by the three methods are clearly distinct and this measure seems more effective in measuring the performance of threshold algorithms when applied to MR-T2 brain images. A higher value of the shape accuracy measure corresponds to a better distinguish of the interior brain regions.

The proposed fuzzy algorithm has certain limitations. The slices used may not fully represent the diversity of T2-weighted MRI axial brain images. Expanding the application to other MRI axial brain datasets could enhance the generalizability of our results. For future work, we plan to reduce the computational cost of the algorithm through code optimization, and make the performance of the algorithm independent of the images' histogram characteristics.

Table 3. Comparison of threshold values

Testing images	Proposed method	Otsu's method	Kittler method
slice #22	22	59	2
slice #32	94	61	2
slice #42	96	61	2
slice #52	82	57	2
slice #62	90	59	2
slice #72	80	57	3
slice #82	86	55	3
slice #92	82	53	3
slice #102	79	52	2
slice #112	89	52	2

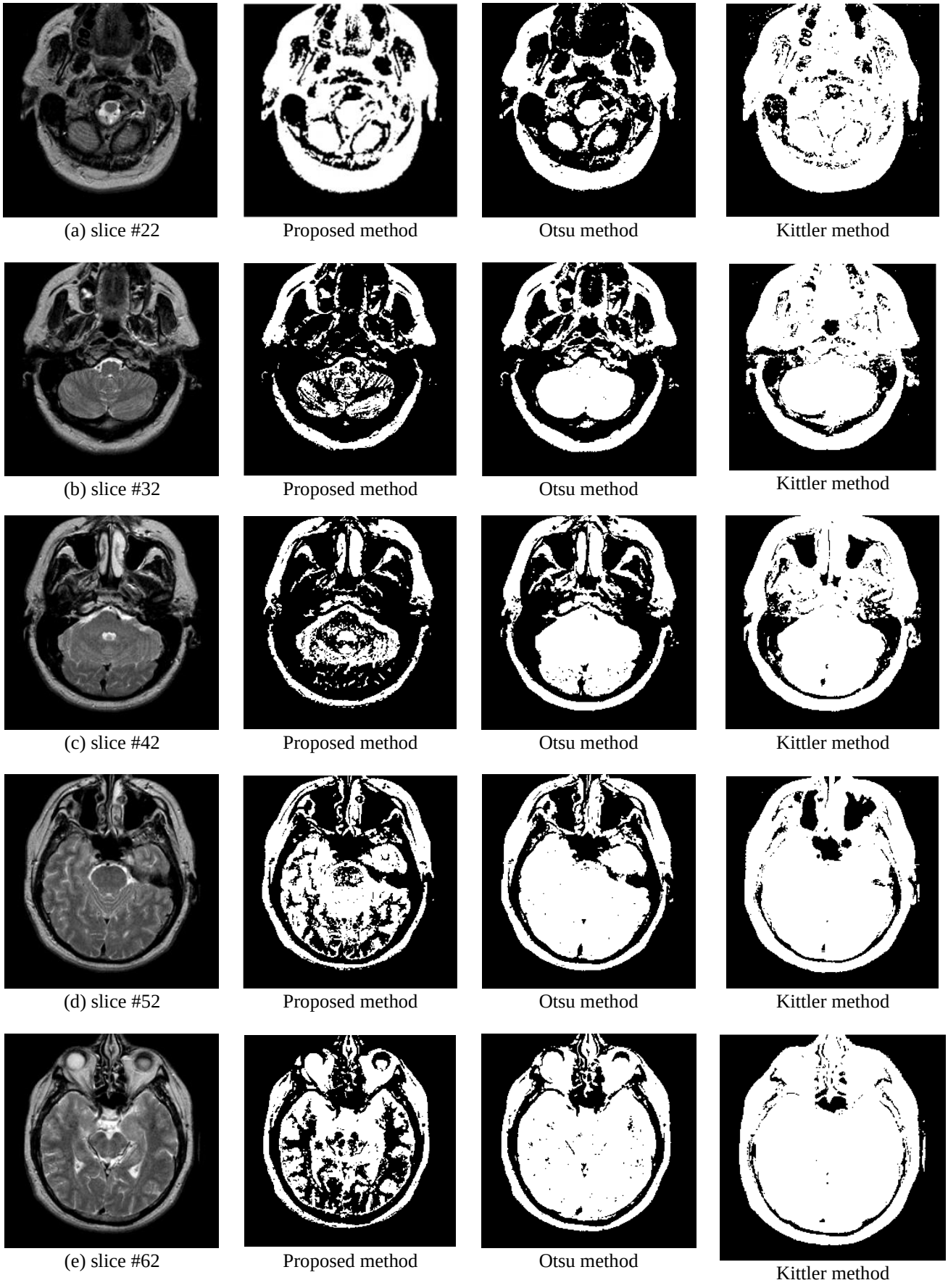

(a) slice #22 Proposed method Otsu method Kittler method

(b) slice #32 Proposed method Otsu method Kittler method

(c) slice #42 Proposed method Otsu method Kittler method

(d) slice #52 Proposed method Otsu method Kittler method

(e) slice #62 Proposed method Otsu method Kittler method

Fig. 7. *(continues on next page)*

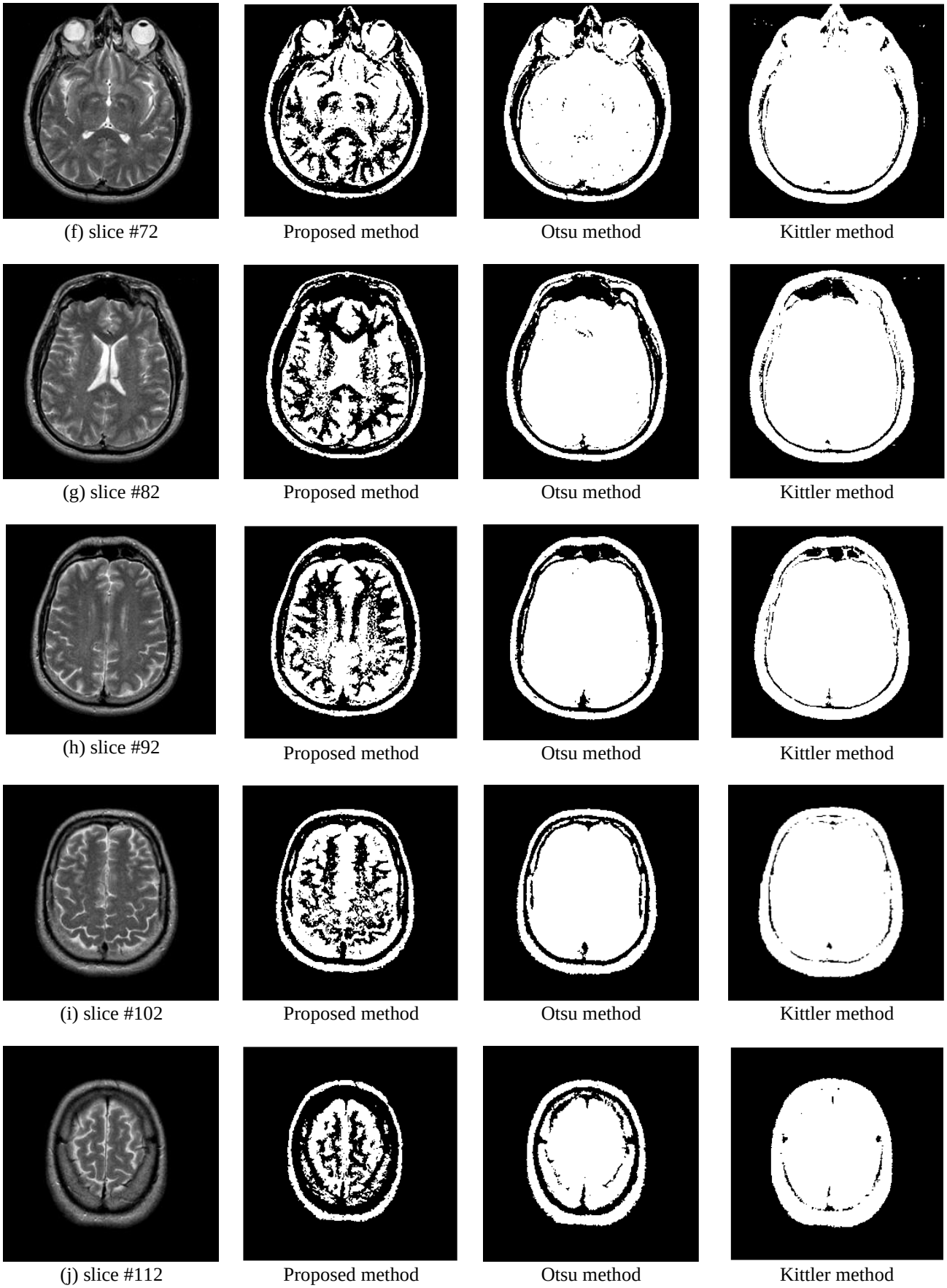

Fig. 7. Segmentation results of brain slices #22 - #112.

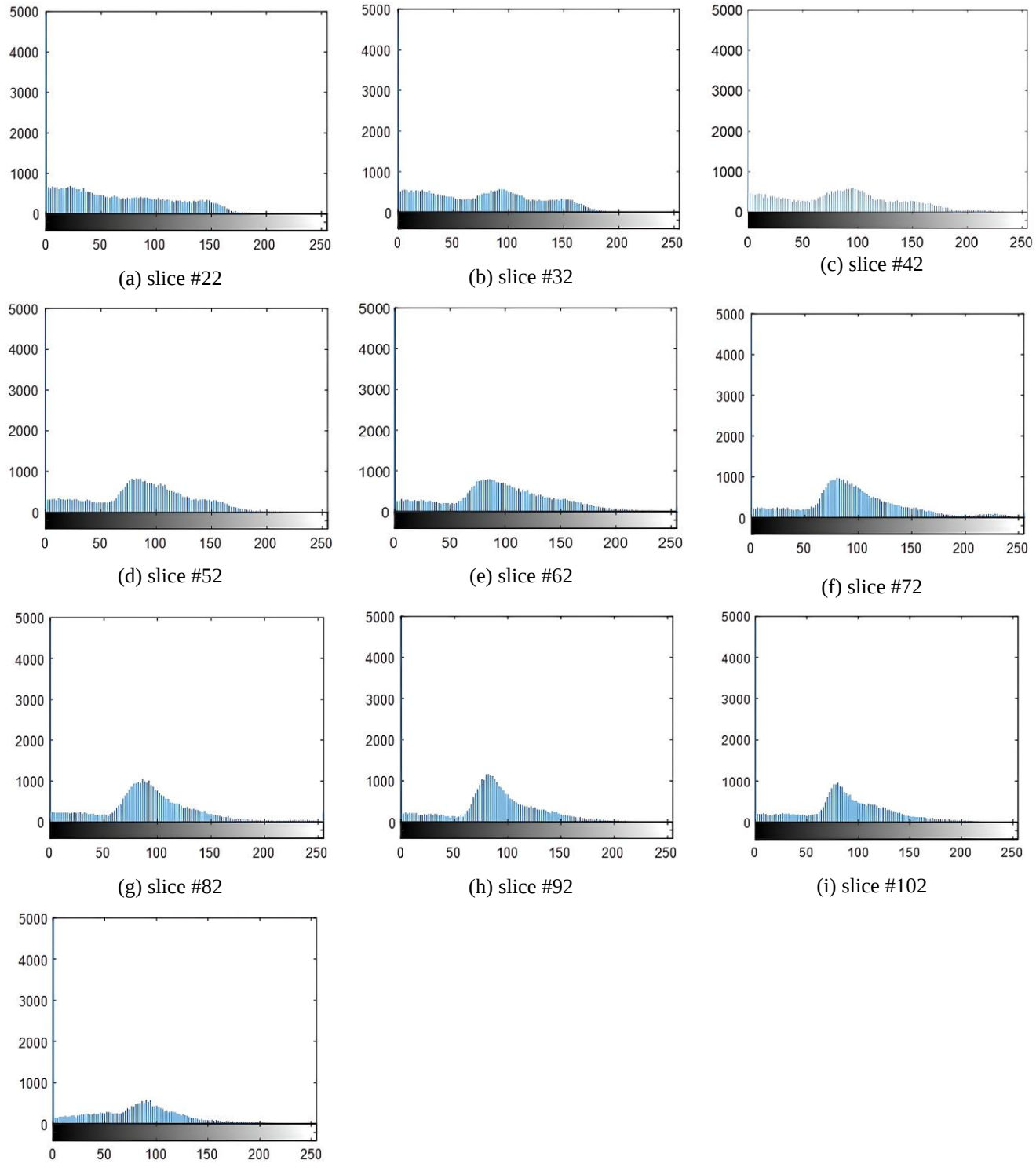

(a) slice #22 (b) slice #32 (c) slice #42

(d) slice #52 (e) slice #62 (f) slice #72

(g) slice #82 (h) slice #92 (i) slice #102

(j) slice #112

Fig. 8. Histogram of brain slices #22 - #112.

5. Conclusions

This paper addresses the problem of brain threshold in T2-weighted MRI axial brain images. We proposed a new automatic thresholding method for gray level brain MRI based on modified type-2 fuzzy compactness. Experiments were done using MRI medical images from the Harvard Medical School that are freely available. For the analyses of the proposed method effectiveness, it was performed a comparison of the obtained results with the correspondent ones obtained with the Otsu and Kittler methods. For the accuracy measure it was used the uniformity and shape measures. From this study, it was possible to conclude that the proposed method performs a state-of-the-art result for a bimodal gray-level histogram and if one demands better shape

of the object in the binary image. The Otsu method is slightly better thresholding method if the gray-level histogram it is not clearly bimodal and for a more uniformity object in the binary image. In the used MRI-T2 brain images the Kittler method is not very effective in the thresholding selection because the criterion function used by that method found a local minimum in the boundaries of the interval of the gray level values of the images. In image processing area the image thresholding is a difficult task and maybe we will never find an algorithm that have a better performance to all types of images. Therefore, it is convenient to search for new thresholding techniques and the type-2 fuzzy sets provide an increase of flexibility in their membership functions that permit to obtain an optimal threshold value.

Acknowledgment

This work was supported by national funds through FCT – Fundação para a Ciência e a Tecnologia, under project UID/CEC/50021/2019 and UIDB/50021/2020.

References

[1] J. Ringenberg, M. Deo, V. Devabhaktunia, O, Berenfeldc, P. Boyersd, J. Gold, "Fast, accurate, and fully automatic segmentation of the right ventricle in short-axis cardiac MRI", Computerized Medical Imaging and Graphics, vol. 34, 2014, pp. 190-201.

[2] A. Memis, S. Varli, F. Bilgili, "Semantic segmentation of the multiform proximal femur and femoralhead bones with the deep convolutional neural networks in low quality MRI sections acquired in different MRI protocols", Computerized Medical Imaging and Graphics, vol. 81, 2020, pp. 1-18.

[3] J. Cousty, L. Najman, M. Couprie, S. Clément-Guinaudeau, T. Goissen, J. Garot, "Segmentation of 4D cardiac MRI: Automated method based on spatio-temporal watershed cuts", Image and Vision Computing, 28, 2010, pp. 1229-1243.

[4] J. Lázaro, J.L. Martín, J. Arias, A. Astarloa, C. Cuadrado, "Neuro semantic thresholding using OCR software for high precision OCR applications", Image and Vision Computing, 28, 2010, pp. 571-578.

[5] Y. Feng, H. Zhao, X. Li, X. Zhang, H. Li, "A multi-scale 3D Otsu thresholding algorithm for medical image segmentation", Digital Signal Processing, Vol. 60, Elsevier, January 2017, pp. 186-199.

[6] U. Ilhan, A. Ilhan, "Brain tumor segmentation based on a new threshold approach", Procedia Computer Science, 102, 2017, pp. 580-587.

[7] M.R. Seshan Ram, M. Balasubramanian, "A comparative analysis on multilevel thresholding of medical image segmentation using social spider and bacterial foraging algorithms", International Journal of Pure and Applied Mathematics, Vol. 119, Nº. 14, 2018, pp. 515-525.

[8] M. Maitra, A. Chatterjee, "A novel technique for multilevel optimal magnetic resonance brain image thresholding using bacterial foraging", Measurement, Elsevier, Vol. 41, pp. 1124–1134, 2008.

[9] T. Kalaiselvi, P. Nagaraja, V. Indhu, "A comparative study on thresholding techniques for gray image binarization", International Journal of Advanced Research in Computer Science, Vol. 8, Nº. 7, 2017.

[10] J. Minnema, M. Eijnatten, W. Kouw, F. Diblen, A. Mendrik, J. Wolff, "CT image segmentation of bone for medical additive manufacturing using a convolutional neural network", Computers in Biology and Medicine, 103, 2018, pp. 130-139.

[11] N. Senthilkumaran, S. Vaithegi, "Image Segmentation by using Thresholding Techniques for Medical Images", Computer Science & Enginnering, Vol. 6, nº.1, 2016.

[12] K. Sudharani, T. C. Sarma, K. Satya Prasad, "Histogram Related Threshold Technique for Region based Automatic Brain Tumor Detection", Indian Journal of Science and Technology, Vol. 9, No. 48, 2016.

[13] H.R. Tizhoosh, "Image Thresholding using type II fuzzy sets", Pattern Recognition, vol. 38, pp.2363-2372, 2005.

[14] P. Kaur, T. Chaira, "A novel fuzzy approach for segmenting medical images", Soft Computing, Vol. 25, pp. 3565–3575, 2021.

[15] T. Sharma, N.K. Verma, "Adaptive Interval Type-2 Fuzzy Filter: An AI Agent for Handling Uncertainties to Preserve Image Naturalness", IEEE Transactions on Artificial Intelligence, Vol. 2, Issue: 1, pp. 83-92, 2021.

[16] P. Murugeswari, S. Vijayalakshmi, "A New Method of Interval Type-2 Fuzzy-Based CNN for Image Classification", Computational Vision and Bio-Inspired Computing, pp. 733-746, 2021.

[17] S. Huang, G. Zhao, Z. Weng, S. Ma, "Trapezoidal type-2 fuzzy inference system with tensor unfolding structure learning method", Neurocomputing, Vol. 473, pp. 54-67, 2022.

[18] T. Chaira, "Edge detection of mammogram images using Pythagorean fuzzy set and Type 2 fuzzy set–an innovative approach", The Imaging Science Journal, 2024.

[19] A. Mohammadzadeh, C. Zhang, K.A. Alattas, F.F.M. El-Sousy, M.T. Vu, "Fourier-based type-2 fuzzy neural network: Simple and effective for high dimensional problems", Neurocomputing, 547, 126316, 2023.

[20] P. Shamoi, M. Muratbekova, A. Izbassar, A. Inoue, H. Kawanaka, "Towards a Universal Understanding of Color Harmony: Fuzzy Approach", Computer Vision and Pattern Recognition, arXiv:2310.00791, 2023.

[21] A. Roselfeld, "The fuzzy geometry of image subsets", Pattern Recognition Letters, vol. 2, issue 5, pp. 311-317, 1984.

[22] L.A. Zadeh, "Calculus of fuzzy restrictions", Fuzzy Sets and Their Applications to Cognitive and Decision Processes. Academic Press, London, pp. 1-39, 1975.

[23] H. Zhang, J.E. Fritts, S.A. Goldman, "Image segmentation evaluation: A survey of unsupervised methods", Computer Vision and Image Understanding, Vol. 110, No. 2, pp. 260–280, 2008.

[24] J.S. Cardoso, L. Corto-real, "Toward a generic evaluation of image segmentation", IEEE Trans. on Image Processing, Vol. 14, No. 11, pp. 1773-1782, 2005.

[25] D. Bradley, G. Roth, "Adaptive Thresholding using the Integral Image", Journal of Graphics, GPU, and Game Tools, Vol. 12, nº.:2, pp. 13-21, 2007.

[26] J.M. White, G.D. Roher, "Image Thresholding for Optical Character Recognition and Other Applications Requiring Character Image Extraction", IBM Journal of Research and Development, Vol. 27, Nº. 4, 1983, pp. 400-411.

[27] M. D. Levine and A. M. Nazif, "Dynamic measurement of computer-generated image segmentation", IEEE Transactions on Pattern Analysis and Intelligence, vol. PAMI-7, no. 2, pp. 155-164, 1985.

[28] C. Li, J.C. Gore, C. Davatzikos, "Multiplicative intrinsic component optimization (MICO) for MRI bias field estimation and tissue segmentation", Magn. Reson. Imaging, Vol. 32, No. 7, pp. 913–923, 2014.

[29] S. Manikandan, K. Ramar, M.W. Iruthayarajan, "Multilevel thresholding for segmentation of medical brain images using real coded genetic algorithm", Measurement, Vol. 47, pp. 558–568, 2014.

[30] P.D. Sathya, R. Kayalvizhi, "Optimal segmentation of brain MRI based on adaptive bacterial foraging algorithm", Neurocomputing, Vol. 74, No. 14, pp. 2299–2313, 2011.

[31] P. K. Sahoo, S. Soltani and A. K. C. Wong, "A survey of thresholding techniques", Computer Vision, Graphics, and Image Processing, vol. 41, no. 2, pp. 233-260, 1988.

[32] C. I. Chang, Y. Du, J. Wang, S.M. Guo and P.D. Thouin, "Survey and comparative analysis of entropy and relative entropy thresholding techniques", IEE Proceedings - Image and Signal Processing, vol. 153, no. 6, pp. 837-850, 2006.

[33] F. Nie F, C. Gao, Y. Guo, M. Gan, "Two-dimensional minimum local cross-entropy thresholding based on co-occurrence matrix", Computers & Electrical Engineering, vol. 37, no. 5, pp. 757-767, 2011.

[34] C.-I Chang, Y. Du, J. Wang, S.-M. Guo, P. D. Thouin, "Survey and comparative analysis of entropy and relative entropy thresholding techniques", IEE Proc. Vision, Image and Signal Processing, vol. 153, no. 6, pp. 837-850, 2006.

[35] F. Nie F, X. Wang, S. Yu, Z. Liao, "Image Thresholding by Minimizing Tsallis Divergence Measure", International Journal of Signal Processing, Image Processing and Pattern Recognition, vol. 8, no. 8, pp. 89-98, 2015.

[36] http://www.med.harvard.edu/AANLIB/cases/caseNA/pb9.htm.

[37] R. Meegama, "Fully Automated Peeling Technique for T1-Weighted, High-Quality MR Head Scans", International Journal of Image and Graphics, Vol. 4, No. 2, pp.141-156, 2004.

[38] N. Otsu, "A Threshold Selection Method from Gray-Level Histograms", IEEE Transactions on Systems, Man, and Cybernetics, Vol. 9, No. 1, pp. 62-66, 1979.

[39] J. Kittler, J. Illingworth, "Minimum Error Thresholding", Pattern Recognition, Vol. 19, No. 1, pp. 41-47, 1986.

[40] M. Sezgin, B. Sankur, "Survey over image thresholding techniques and quantitative performance evaluation", Journal of Electronic Imaging, Vol. 13, No. 1, pp. 146-165, 2004.

[41] J. Kittler, J. Illingworth, "On threshold selection using clustering criteria", IEEE Trans. Syst. Man. Cybernet. SMC-15, 1985.